Received: 23 October 2020 | Revised: 22 December 2020 | Accepted: 4 January 2021

DOI: 10.1002/nano.202000207

RESEARCH ARTICLE

Nano Select Open Access WILEY

Single cell temperature probed by Eu^{+3} doped TiO_2 nanoparticles luminescence

Maja Garvas[1] | **Selene Acosta**[4] | **Iztok Urbančič**[1] | **Tilen Koklič**[1] | **Janez Štrancar**[1] | **Luiz A. O. Nunes**[2] | **Peter Guttmann**[3] | **Polona Umek**[1] | **Carla Bittencourt**[4]

[1] Jožef Stefan Institute, Ljubljana 1000, Slovenia

[2] Instituto de Física de São Carlos, Universidade de São Paulo, São Carlos, São Paulo, Brazil

[3] Department X-ray Microscopy, Helmholtz-Zentrum Berlin für Materialien und Energie GmbH, Berlin D-12489, Germany

[4] Chimie des Interactions Plasma–Surface (ChIPS), Research Institute for Materials Science and Engineering, Université de Mons, Mons, Belgium

Correspondence
Selene Acosta, Chimie des Interactions Plasma–Surface (ChIPS), Research Institute for Materials Science and Engineering, Université de Mons, Mons, Belgium.
Email: Selene.ACOSTAMORALES@umons.ac.be

Abstract

Temperature is a critical parameter in biology, affecting the speed of reactions that occur in living systems. Nevertheless, measuring temperature with sub-cellular resolution (micrometric scale) and reliability remains a challenge to overcome. In this perspective, luminescence nanothermometry is a non-contact technique which aims to measure temperature with a sub-micrometric spatial resolution through the use of nanomaterials whose luminescence is affected solely by changes in temperature. Here, TiO_2 nanoparticles doped with Eu^{+3} ions (Eu^{+3}-TiO_2) are used for sensing temperature differences within single living cells. XRD, XPS, SEM, TEM and NEXAFS analysis allow the determination of the physicochemical characteristics of the Eu^{+3}-TiO_2 nanoparticles and, the variation of the luminescence intensity of the Eu^{+3}-TiO_2 nanoparticles with their temperature is investigated. The successful internalization of Eu^{+3}-TiO_2 nanoparticles in different types of cells is observed. The luminescence of nanoparticles internalized in L929 fibroblast cells is measured when the system is heated in a biological relevant temperature range. Making use of an appropriate calibration curve the temperature variation inside the cells is determined with sensitivity of 0.5 K per 1% of luminosity change when heated.

KEYWORDS
luminescence, nanoparticles, synchrotron radiation, TiO_2

1 | INTRODUCTION

The determination of temperature is crucial in multiple scientific research fields. In the case of biological systems, temperature plays a very important role as small variations in temperature influence properties and dynamics of biomolecules, affecting the speed of reactions that occur in living systems. For example, proteins experience a structural change and may lose their native structure if the temperature varies a few degrees around 37°C; thus, possible changes in their function can occur.[1] Multiple cellular processes are also regulated by temperature, such as cell division, membrane lipid compositions and gene expression.[2–4] Due to this strong influence of

temperature on biological systems it is important to monitor the temperature while researching the dynamics and properties of cellular systems. In addition to this basic concern, monitoring cellular temperature is also relevant in biomedicine. Cancerous cells were reported to be warmer by few degrees than normal cells due to their higher metabolic activity.[5–7] Following this discovery, temperature sensing in cells can become an important early cancer detection technique. However, measuring the temperature of living cells requires a subcellular spatial resolution as well as a sub-degree thermal resolution which are impossible to achieve with conventional thermometers, such as thermocouples or infrared thermometers.[8,9] In this perspective, luminescence nanothermometry emerges as a promising technique for measuring temperature of systems with a sub-micrometric size that might be capable of achieving the spatial and temperature resolution expected.

Luminescence is the emission of light that occurs following the excitation of electronic states. The properties of the emitted photons depend on the electronic states involved and in certain cases on the local temperature.[10] Luminescence nanothermometry uses the correlation between temperature and luminescence for temperature sensing through variation in the emission spectrum of a luminescent object.[10] Essentially, the temperature value is obtained by evaluating changes in luminescent properties such as absolute and relative emission intensities, excited state lifetime values, peak position and/or emission bandwidth.[11] For systems that do not possess naturally luminescence temperature dependence (such as live cells or electrical devices) it is necessary to conjugate the system of interest with probes whose luminescence is temperature dependent.[12,13] Luminescent temperature probes include organic dyes, polymers, semiconductor nanocrystals, nanogels and trivalent lanthanide (Ln^{+3}) ions as optical centres.[14–19] In this context, lanthanide (Ln^{+3}) doped materials are probes with high potential, due to their narrow and intense luminescent bands, stability in harsh chemical environments, and because their luminescence intensity and lifetime luminescence depends critically on temperature.[20–22] Lanthanides ions also offer a wide range of working temperatures depending on the type of used lanthanide.[23] Transition metal oxides matrices, specially TiO_2 and ZrO_2, are reported to be optimal hosts for lanthanides as a result of their low phonon frequencies and transparency in the visible-NIR region of the spectrum.[24] Furthermore, TiO_2 biocompatibility has been extensively tested in multiple studies giving favorable results, making TiO_2 an optimal host matrix if biological applications are aimed.[25–27] Besides, europium and europium-based nanoparticles also show low cytotoxicity.[28–32] And, Eu^{3+}-doped TiO_2 nanoparticles were tested in biomedical applications for two-phonon imaging of cancer cells (HeLa) and for time resolved fluoroinmuno-assay in human PSA.[33.34]

In this study, we evaluated TiO_2 nanoparticles doped with Eu^{+3} ions as nanothermometers for single cell temperature measurement. This work was performed monitoring the variation of luminescence intensity of the $^5D_0 \rightarrow {}^7F_j$ (j = 0, … 6) emissions for increasing sample temperature.[11] The luminescence of Eu^{+3}-TiO_2 was acquired in the biological relevant temperature range of 20-40°C. Before thermal sensing, the Eu^{+3}-TiO_2 nanoparticles were characterized by X-ray Photoelectron Spectroscopy (XPS), X-ray Diffraction (XRD), Nanoscale Near Edge X-Ray Absorption Fine Structure (NEXAFS-TXM), Scanning Electron (SEM) and Transmission Electron (TEM) Microscopies. The internalization of Eu^{+3}-TiO_2 nanoparticles in cells was evaluated in a mouse lung epithelial cells (LA–4), and mouse fibroblast cells (L929). The evaluation of the temperature of cells through luminescence nanothermometry was performed in the L929 fibroblast cells.

2 | RESULTS AND DISCUSSION

2.1 | Characterization of the Eu^{+3} -TiO_2 nanoparticles

TiO_2 nanoparticles doped with 1, 3 and 5 wt. % of Eu^{+3} were synthesized by the sol-gel method. The synthesized samples were firstly characterized to determine their phase composition, morphology, nanoparticle size, doping level, surface chemical composition and their luminescence yield. The X-ray powder diffraction (XRD) spectra of all three synthesized samples (1, 3 and 5 wt. % of Eu^{+3}) match up with anatase phase (ICDD card no. 78–2486).[35] Figure 1A shows the XRD pattern of 5%Eu^{+3}-TiO_2. No diffraction peaks belonging to Eu_2O_3 were observed in the XRD patterns of all three samples. The XPS measurements show that sample surfaces are composed of titanium, oxygen, europium and carbon atoms (Figure 1B). The presence of carbon in the spectrum can be associated with adventitious carbon contamination from ambient exposure. Results of SEM and TEM characterization of the 5%Eu^{3+}-doped TiO_2 sample are presented in Figure 2. SEM image (Figure 2A) reveals that the as prepared material is strongly agglomerated (ultrasound sonication was not used for sample preparation); the agglomerates do no exceed 500 nm. Before TEM imaging (Figure 2B) the sample was sonicated which significantly reduced the size of the agglomerates, the smallest aggregates are composed of two to five crystallites with diameters between 15 and 20 nm (see the white arrows at Figure 2B) and thus have the right size to be internalized by different types of cells. The europium content (wt. %) determined with EDX

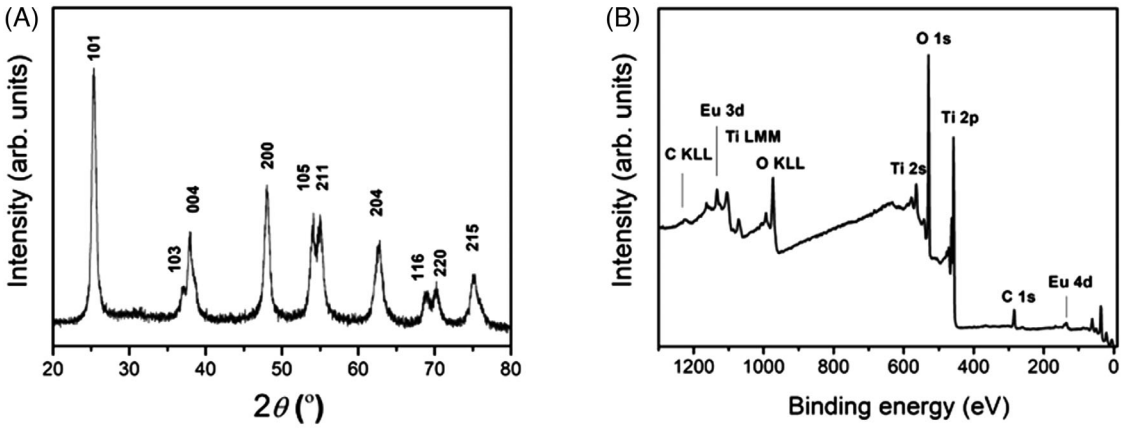

FIGURE 1 A, X-ray powder diffraction (XRD) spectrum of 5%Eu^{+3}-TiO_2. All peaks are indexed to anatase TiO_2 structure (ICDD card no. 01-78-2486). B, X-ray photoelectron spectrum (XPS) of 5%Eu^{+3}-TiO_2

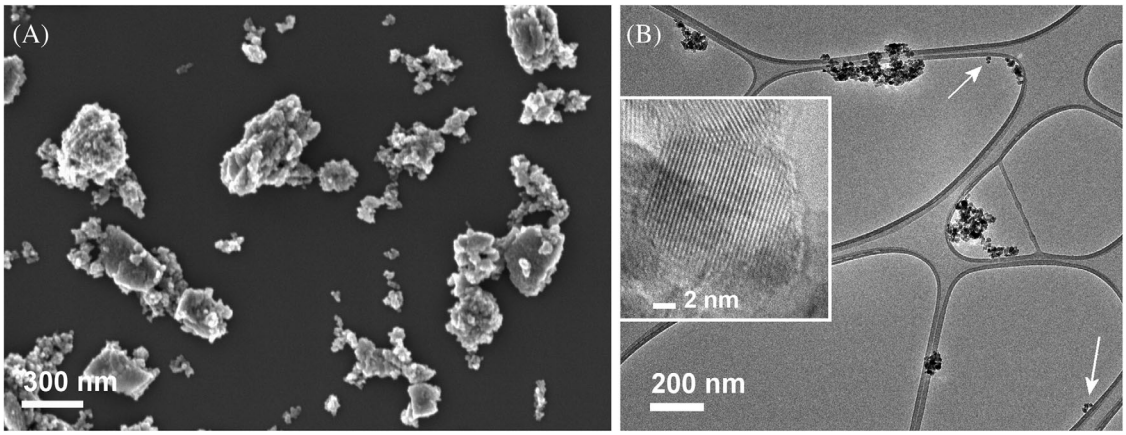

FIGURE 2 SEM (A) and TEM (B) microscopy images of 5%Eu^{+3}-TiO_2 sample. TiO_2 nanoparticles are crystalline (inset to figure (B)) with diameters between 15 and 20 nm. They form agglomerates and their size does not exceed 500 nm. Small agglomerates (white arrows) composed of two to five nanoparticles are also observed

was 0.8 ± 0.2 (1%Eu^{+3}-TiO_2), 3.0 ± 0.4, (3%Eu^{+3}-TiO_2) and 4.1 ± 0.8, (5%Eu^{+3}-TiO_2).

The NEXAFS spectra of the Ti L-edge, and O K-edge recorded on the samples (Figure S1), show the fingerprint of the anatase phase in agreement with the XRD results (Figure 1A).[36] The NEXAFS measurements recorded on the Eu M-edge indicate that europium ions in all three samples have essentially the oxidation state Eu^{+3} (Figure S2). All three samples show luminescence properties; however, for the temperature measurements only the sample 5%Eu^{+3}-TiO_2, which has the highest luminescence yield, was used. The luminescence spectra of 5%Eu^{+3}-TiO_2 measured as a function of temperature (15-50°C) are shown in Figure S3. The emission of the Eu^{+3} dopant ions, at the low energy spectral region, is composed of characteristic bands that arise from transitions of the first excited level of Eu^{+3} ($^5D_0$) to the ground state multiplets ($^7F_0$, $^7F_1$, $^7F_2$, and $^7F_3$). We observed that the luminescence intensity of the Eu^{+3} emission is very sensitive to temperature variation, decreasing for increasing temperatures, this behavior is associated to an increase in non-radiative relaxation processes, due to thermal population of the ground state ($^7F_0$, $^7F_1$, $^7F_2$, and $^7F_3$).[11]

2.2 | Eu^{+3}-TiO_2 nanoparticles incubation in cells

To verify the applicability of the 5%Eu^{+3}-TiO_2 nanoparticles to evaluate the temperature variation in living cells, mouse fibroblasts L929 were used as a test organism and several in vitro experiments were done. The internalization of the nanoparticles in mouse fibroblasts was evaluated with combination of different optical microscopy techniques: microscope operating in bright-field mode, fluorescence imaging mode, and fluorescence

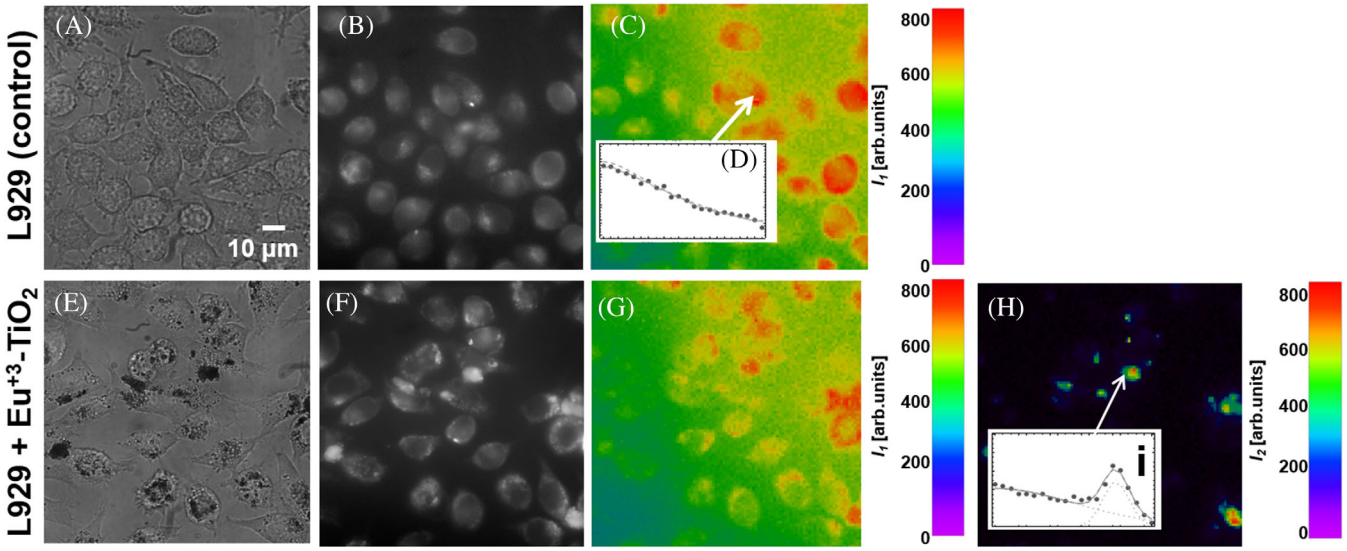

FIGURE 3 A, Brightfield and (B) widefield autofluorescence images of L929 fibroblasts cells. C, Fluorescence microspectroscopy image of (B). D, Typical autofluorescence emission spectrum from control cells. E, Brightfield image of L929 cells incubated with 5 wt.% Eu^{+3}-TiO_2 nanostructures for 2 days. F, Widefield fluorescence microscopy image of the same area shown in (E). G, Fluorescence microspectroscopy image – color coded by autofluorescence component from cells. H, fluorescence microspectroscopy image – luminescence of the europium component. Images (C), (G) and (H) are color coded by fluorescence and luminescence intensity (purple – low; red – high intensity), respectively. I, Emission spectrum obtained from incubated cells: autofluorescence (left region – linear) and europium luminescence (right region – Gaussian-Loretzian) are present. 430-460 nm excitation, 495 nm dichroic and 523-643 nm emission filter setup was used with 5 nm scan step. All images have the same scale bar

microspectroscopy mode. First, we obtained a set of images of control cells (no nanoparticles incubated) with the aim to determine cell autofluorescence (Figure 3A – brightfield image, B – fluorescence). Indeed, the autofluorescence signal of the L929 cells is very intense (Figure 3B – fluorescence) rendering detection of the Eu^{+3}-TiO_2 nanoparticles emission impossible. However, since the Eu^{+3}-TiO_2 nanoparticles have a very sharp emission peak at 615 nm (Figure S3) it is possible to distinguish the nanoparticles' emission from the cell autofluorescence signal employing optical microscopy in microspectroscopy mode. We, therefore, also recorded fluorescence emission spectrum in each pixel of the fluorescence image. An example of fluorescence emission spectrum is shown in Figure 3D, the emission spectrum was fitted as described previously in Arzov et al. 2011 and its intensity is plotted in Figure 3C (Figure 3C – autofluorescence component).[37] Brightfield images of cells after 2 days of incubation with Eu^{+3}-TiO_2 nanoparticles reveal several dark areas located at same places as cells (Figure 3E – brightfield), suggesting that Eu^{+3}-TiO_2 nanoparticles are either located inside the cells or adsorbed at their surface. Although several bright areas appear in the fluorescence image one cannot be sure that they originate from the Eu^{+3}-TiO_2 nanoparticles (Figure 3F – fluorescence). However, in the fluorescence microspectroscopy mode, the fluorescence emission spectrum can be decomposed in each pixel of the fluorescence image in two components: one corresponding to cell autofluorescence (Figure 3G – autofluorescence component) and a second component corresponding to emission from the Eu^{+3}-TiO_2 nanoparticles (Figure 3H – Eu^{+3}-TiO_2 nanoparticles component). In this way we can clearly locate the nanoparticles, and show that luminescence of Eu^{+3}-TiO_2 nanoparticles occurs at the same position as cells autofluorescence signal; therefore, indicating that the nanoparticles are co-localized or are in close proximity to the cells. An emission spectrum showing the characteristic Eu^{+3} emission peak at 615 nm is detected in different cell areas when cells are incubated with nanoparticles (Figure 3I). The broad spectral component of the emission spectrum corresponds to cell autofluorescence (Figure 3D – autofluorescence emission spectrum) whereas the narrow component of the spectrum shows the europium luminescence band centered at 615 nm (Figure 3I – Eu^{+3}-TiO_2 emission spectrum superimposed with autofluorescence spectrum). The luminescence band is not observed in the spectrum recorded on the sample where cells were not incubated with nanoparticles (Figure 3D).

Additional experiments were done to verify the successful internalization of Eu^{+3}-TiO_2 nanoparticles in L929 fibroblast, they are shown in the supplementary data (Figures S4 and S5). To determine whether the nanoparticles are internalized within the cells or adsorbed to their surface the confocal fluorescence mode with better

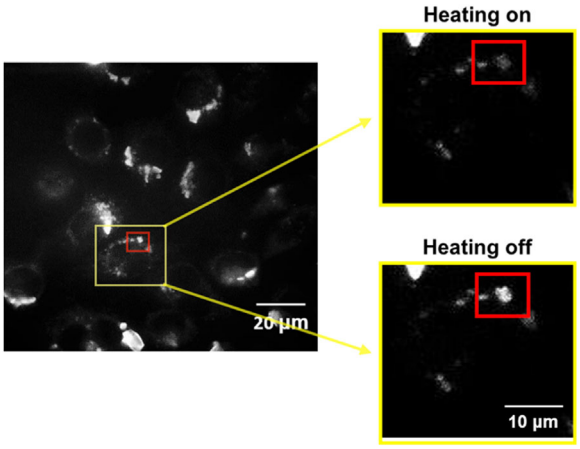

FIGURE 4 Fluorescence widefield microscopy image of 5%Eu^{+3}-TiO_2 nanoparticles internalized in L929 fibroblasts cells. Red rectangle indicates an area that was heated with infrared heating laser (1064 nm, 200 mW, focal point less than 1 µm). The images were recorded when the sample was at room temperature or was heated (shown in zoom). The magnified image above corresponds to the heated sample (heating laser turned on for 5 seconds), and the magnified image bellow correspond to the sample at room temperature (heating laser turned off for 10 seconds). It can be observed that when the heating laser is turned on the intensity of luminescence decreases, this effect is associated to an increase in non-radiative relaxation processes. 430-460 nm excitation, 495 nm dichroic and 523-643 nm filter setup was used. Magnified images have the same scale bar

spatial resolution was used. The internalization of Eu^{+3}-TiO_2 nanoparticles (Figure S6A) with different morphologies (spherical and tubes) in lung mouse epithelial LA–4 cells was confirmed (Figure S6B). Note the vertical cross section in Figure S6A, C and D clearly shows that the internalization of the Eu^{+3}-TiO_2 nanoparticles depends neither on the nanoparticle morphology nor on the cell type. These results support the suggestion that Eu^{+3}-TiO_2 nanoparticles with different morphologies have potential to internalize into different cell lines.

2.3 | Variation with temperature of Eu^{+3}-TiO_2 luminescence in mouse fibroblast cells

Fluorescence/Luminescence images of Eu^{+3}-TiO_2 internalized in L929 fibroblast cells were recorded using a set of filters (430-460 nm excitation, 495 nm dichroic and 523-643 nm emission) (Figure 4). The bright spot inside the area limited by the red rectangle are Eu^{+3}-TiO_2 nanoparticles. When the particles are heated using an infrared laser (1064 nm, 200 mW, focal point less than 1 µm), their luminescence intensity drops. Based on the obtained data we can ascertain that the decrease in the luminescence intensity corresponds to the increase in the local temperature.

In order to use the Eu^{+3}-TiO_2 nanoparticles as nanothermometers for detection of temperature variation inside living cells, we calibrated the variation of the fluorescence intensity of the 5%Eu^{+3}-TiO_2 nanoparticles with variation of the temperature. Considering that water is the main abundant molecule in cells, accounting for 70% of total cell mass, we used dispersed Eu^{+3}-TiO_2 particles in distilled water simulating cell internalized particles and we obtained the luminescence spectra at different temperatures in the biological relevant range with an excitation of 430-460 nm; the emission transitions $^5D_0$ – ^4F_j (j = 0,1,2,3,4) are observed (Figure 5A), an energy level diagram with the transitions involved is showed in Figure S7. The temperature calibration was performed using the fluorescence microscope by heating the whole replicate sample using an objective-ring, placed on a water immersion objective, which can heat up the sample precisely enough without severe vertical gradients. We used 430-460 nm excitation, 495 nm dichroic and 580-643 nm emission filters. The temperature calibration curve was obtained integrating the luminescence intensity in each pixel of the image recorded at a chosen temperature. To verify the calibration curve we also measure the luminescence at three different temperatures using a spectrofluorometer, (Figure 5A) and the intensity at the peak maximum on 615 nm was used. The calibration curve (Figure 5B) was used for transformation of the fluorescence intensity in temperature difference (ΔT). When temperature increased the luminescence intensity decreased through the whole spectral range. The temperature calibration curve of the heated Eu^{+3}-TiO_2 nanoparticles revealed the sensitivity of the Eu^{+3} doped nanoparticles as nanothermometers, that is, when the luminescence intensity of the nanoparticle decreases by 1 percent () the nanothermometer can detect temperature difference of (Figures S9 and S10).

Using the obtained calibration curve, we evaluated the temperature changes in cells using the internalized 5%Eu^{+3}-TiO_2 nanoparticles luminesce intensity variation when the sample (L929 fibroblasts incubated with nanoparticles) was heated (Figure 6). The luminescence intensity variation of internalized nanoparticles in L929 fibroblasts was analyzed at three different areas of cells: light blue and blue rectangles limit a non-heated area of the sample while the green rectangle limits the heated internalized nanoparticle (Figure 6A,B). Using the calibration curve in Figure 5B, we can determine the local temperature variation of the internalized nanoparticle when the sample was heated using an infrared laser. The temperature variation curve is described by Equation 1.

$$\Delta T = a \cdot \Delta I \quad (1)$$

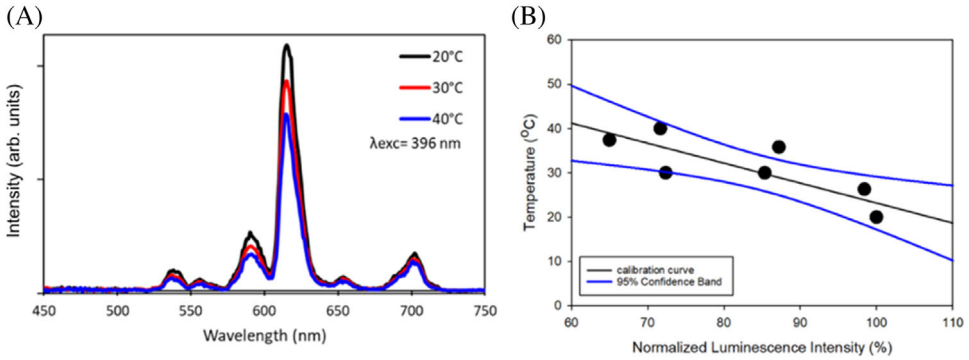

FIGURE 5 A, Luminescence spectra of 5%Eu^{+3}-TiO_2 nanoparticles taken at different temperatures obtained with spectrofluorometer. B, Calibration curve of variation of temperature versus normalized luminescence intensity obtained in a water dispersion of Eu^{+3}-TiO_2 nanoparticles. The nanoparticles dispersion was heated to reach different temperatures. Luminescence intensity of the emitted light was measured using either a fluorescence microscope (heated to reach different temperatures with an objective-ring) or a spectrofluorometer (both data represented with black circles), since both data were overlapping they were fitted together with a linear function (black solid line). We used 430-460 nm excitation, 495 nm dichroic and 580-643 nm emission filters

where $a = (-0.45 \pm 0.12)°C\ \%^{-1}$. Equation 1 is used for the transformation of the luminescence intensity variation (ΔI) (Figure S8) in temperature difference (ΔT). This equation shows the sensitivity of the Eu^{+3} doped nanoparticles as nanothermometers, namely, when luminescence intensity of the nanoparticle decreases by 1 percent ($\Delta I = 1\%$) the nanothermometer can detect temperature difference as indicated in Equation 2.

$$\begin{aligned}\Delta T &= a \cdot \Delta I = (-0.45 \pm 0.12)^{\circ} C \cdot \%^{-1} \cdot (-1\%) \\ &= 0.45°C \pm 0.12°C \end{aligned} \quad (2)$$

In Figure 6C we can see that for the nanoparticle in the heated region of the cell there is an evident luminescence intensity change while no changes are observed for the non-heated area of the sample. Using the calibration curve it is possible to translate the luminescence intensity variation (Figure S8) in temperature variation (Figure 6C), we can observe that an increment of up to 6°C degrees in the cells through the analysis of the luminescence intensity of 5%Eu^{+3}-TiO_2 was observed. Note that only the nanoparticles inside the green area change the intensity of the emitted light when the area is heated with an infrared laser.

3 | CONCLUSION

We observed that Eu^{+3}-TiO_2 nanoparticles are readily internalized in different types of cells and their luminescence as well as their luminescence dependence with temperature variation in the physiological temperature range can be measured even after they are internalized. We demonstrated that TiO_2 nanoparticles doped with Eu^{+3} can be used as highly sensitive nanothermometers to probe temperature variation in living cells. By measuring the luminescence intensity variation of internalized 5%Eu^{+3}-TiO_2 nanoparticles we obtained information about cells temperature variation with sensitivity off $0.45°C \pm 0.12°C$ per 1% change in luminosity. This result opens the possibility of the use of Eu^{+3}-TiO_2 nanoparticles in biomedical technologies as nanothermometers for single cell temperature evaluation. In this perspective, they could potentially be used as thermometers for various cellular organelles, since they can be functionalized with different biomolecules, which might localize them at specific organelles.[27,38] However, specific assays of toxicity and maximum tolerated dose need to be done to evaluate the use of Eu-TiO_2 nanoparticles in more complex living organisms. Although the Eu^{+3}-TiO_2 nanoparticles showed to be a very reliable nanothermometer, as expected for such a stable material in different harsh chemical environment, further studies are needed as cells present a complex cytosolic environment with different properties, such as viscosity, pH as well as ion concentration, that might affect luminescence properties of Eu^{+3}-TiO_2 nanoparticles.

4 | EXPERIMENTAL SECTION

Material synthesis: TiO_2 nanoparticles doped with 1, 3 and 5 wt. % of Eu^{+3} were synthesized according to the sol–gel method reported by Antić et al.[39] In short, a solution of 3.4 mL of deionized water, 350 μL of 65% HNO_3, 20 mL of EtOH and 142.3 mg (1 wt. %) or 435.6 mg (3 wt. %) or 741.3 mg (5 wt. %) of $Eu(NO_3)_3 \cdot 5H_2O$ was added slowly to a solution of 19.2 mL of titanium(IV) isopropoxide and 73 mL of EtOH. Transparent gels were obtained in few minutes and dried first at 70°C for 5 hours. The samples were further heated to 100°C and held at this temperature for

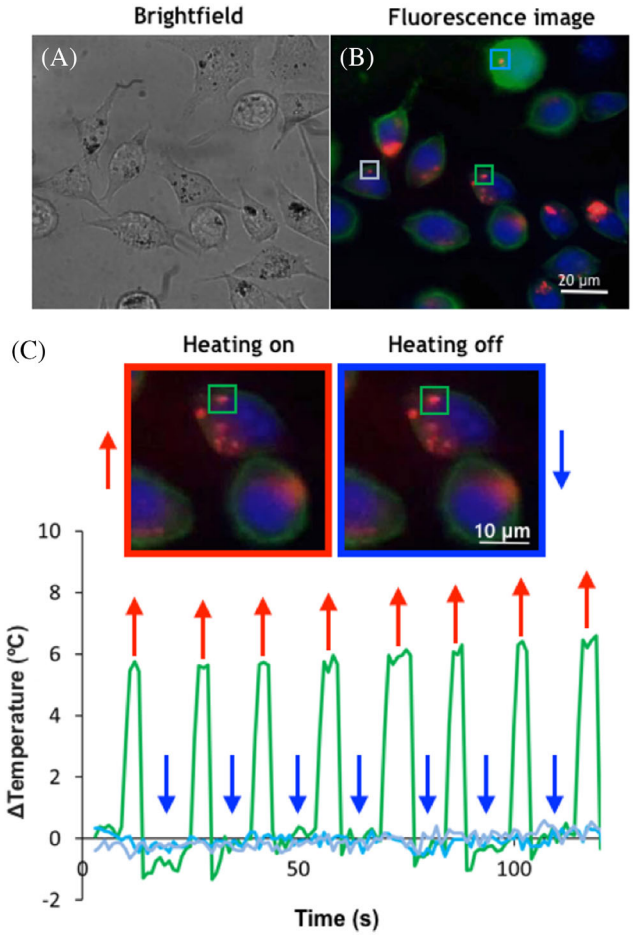

FIGURE 6 A, Brightfield and (B) overlay of three fluorescence widefield microscopy images of L929 fibroblasts incubated with 5%Eu^{+3}-TiO_2 nanoparticles for 3 days (nanoparticles are presented in red, cell nuclei in blue, and plasma membrane in green). Green rectangle indicates an area heated with an infrared laser, whereas blue rectangles indicate nanoparticles also located inside the cells but not heated with the laser (1064 nm, 200 mW, focal point less than 1 µm). Radial distribution of the temperature, that increase due to heating with the IR laser, was measured in a thin layer of ethanol solution and fluorophore (SPP268). Maximal temperature difference was 6°C at the laser beam position, which decreased radially, achieving half of the maximum value at about 20 micrometers from the center and reaches 0 (equal to non-heated background) about 40 micrometers from the center. This agrees with the experimental data and with calculations from the literature, which show that luminescence intensity of nanoparticles in neighboring cells away by more than 50 micrometers does not change (Figure 6B, blue line). [30] C, Local temperature response of the heated nanoparticles (green) and no response of non-heated nanoparticles (blue). Magnified images from an area with heated nanoparticles with evident luminescence intensity variation are shown above the time traces of temperature variation. The filters used in experiments were the following: for the nuclei imaging 352-402 nm excitation, 409 nm dichroic, and 420-520 nm emission filters, for 5%Eu^{+3}-TiO_2 nanoparticles imaging 430-460 nm excitation, 495 nm dichroic and 580-643 nm emission filters were used, and for the membrane imaging 430-460 nm excitation, 495 nm dichroic and 506-594 nm emission filters were used

12 hours, and finally calcined at 450°C for 10 hours. The best luminescence results were observed for the sample synthesized with 5 wt. % of Eu^{+3} (5% Eu-TiO_2); therefore, only the results related to this sample are presented.

Material characterization: The phase composition of the samples was determined with X-ray powder diffraction (XRD), using a D4 Endeavor, Bruker AXS diffractometer with Cu-Kα radiation ($\lambda = 1.5406$ Å) and a Sol-X energy-dispersive detector. Diffractograms were measured in the 2θ angular range between 20° and 80° with the step size of 0.02 $seconds^{-1}$ and the collection time of 3 seconds. The morphology of the samples was investigated with scanning (FE-SEM, Jeol 7600F) and transmission electron microscopes (TEM Jeol 2100, 200 keV). Specimens for SEM characterization were prepared as a water dispersion of the sample; a small amount of the sample was placed in an agate mortar where it was gringed with a small amount of deionized water with a pestle. One drop of the prepared dispersion was placed on a polished Al sample holder. The holder with the dried product was coated with a 3 nm thick carbon layer prior to the SEM investigation. For TEM analyses, the sample was dispersed in methanol and ultrasonicated for 20 minutes. One drop of the dispersion was then deposited on a lacy carbon film supported by a copper grid (300 mesh). The europium content in the samples was determined with FE-SEM equipped with an energy-dispersive X-ray spectrometer (EDXS) elemental analysis system. Specimens for the EDXS analysis were prepared by pressing the samples into pellets, and placing them on a double sided carbon tape on an Al sample holder. The holder with the specimens was coated with a thin carbon layer prior to the EDXS analyses. The chemical composition on the surface of Eu^{+3}-TiO_2 nanoparticles were collected by X-ray photoelectron spectroscopy (XPS) using a VERSAPROBEPHI 5000 from Physical Electronics, equipped with a Monochromatic Al Kα X-ray source. The energy resolution was 0.7 eV. The specimens for XPS measurements were prepared by pressing the sample powders into pellets. A conductive double face tape UHV compatible was used to attach the pellet to a sample holder. The oxidation state of europium in the TiO_2 nanoparticles as well as the confirmation of the crystallization phase of TiO_2 was investigated by Nanoscale Near Edge X-Ray Absorption Fine Structure (NEXAFS). The NEXAFS spectra were collected in the Transmission X-ray Microscope (TXM) installed at the undulator beamline U41-PGM1-XM at the electron storage ring BESSY II, Helmholtz-Zentrum Berlin (HZB).[40–42] The setup of the TXM end station used for this measurement allows analyzing selected regions of the sample with a spatial resolution of 25 nm. The calculated spectral resolution was $E/\Delta E = 10{,}000$. The signal intensity in the proximity of the sample was used to correct variations of the photon flux

with photon energy (hv) and acquisition time. The data analysis was performed using axis2000 (A.P.Hitchock, http://unicorn.mcmaster.ca/aXis2000.html).

Cell culturing: A mouse fibroblast cell line L929 was cultured in a cell medium (DMEM, Sigma-Aldrich) containing 10% of fetal calf serum (FCS, Gibco, ThermoFisher Scientific) and 1% mixture of antibiotics (Penicillin-Streptomycin from Sigma-Aldrich). The cells were cultured at 37°C in a humidified 5% CO_2 atmosphere. For the fluorescence microscopy observation, cells were plated on an 8 well glass-bottom cell culture dish (Lab-Tek Chambred Coverglass) for an additional day.

In order to evaluate the study in different cell types, experiments were also performed using LA-4 murine lung epithelial cells. The LA-4 murine lung epithelial cells were cultured in the complete culturing medium (F12K medium, 15% FCS, 1% Penicillin-Streptomycin (antibiotics), 1% NEAA (nonessential amino acids)). For the fluorescence confocal microscopy observation, cells were plated on an 8 well glass-bottom cell culture dish (iBidi GMBH) for an additional day.

Cells Incubation with Eu^{+3}-TiO_2 nanoparticles: Eu^{+3}-TiO_2 powder was dispersed in two ways: (i) in a complete cell medium with serum and sonicated with a tip sonicator (MISONIX Ultrasound liquid Processor with 419 Microtip TM), with the amplitude set to 70% (power 20-30 W) for t_{run} = 15 minutes, t_{on} = 5 seconds, t_{off} = 5 seconds. Afterwards dispersed nanoparticles were placed for 20 minutes under UV light for sterilization. Final concentration of Eu^{+3}-TiO_2 nanoparticles in the cell medium was 10 mg mL^{-1}, (ii) the powder was dispersed in 1 mM KOH and low ionic straight, sonicated for 20 minutes on a water bath sonicator (BRANSON 2510) and then diluted with complete cell medium to final concentration 100 or 500 μg mL^{-1}.

The cell medium was replaced with the nanoparticles medium dispersion and incubated for additional 2 or 3 days. After the incubation, cells were stained with Hoechst 33342 stain (ThermoFisher Scientific) at nmol concentration for nucleus observation. Membrane fluorophore ((2R,3S,4R,5R,6R)-2-(hydroxymethyl)-5-((7-nitrobenzo[c][1,2,5]oxadiazol-4-yl)amino)-6-((1-tetradecyl-1H-1,2.3-tiazol-4-yl)methoxy)tetrahydro-2H-pyran-3,4-diol) at nmol concentration was added to the cell samples just before imaging.[43] LA-4 cells plasma membrane was labelled with the CellMaskOrange membrane stain (5 μg mL^{-1}, Invitrogen), incubated at room temperature for additional 5 minutes and washed.

Co-localization imaging of lysosomes with 5%Eu^{+3}-TiO_2 nanoparticles (400 or 500 μg mL^{-1}) was performed using a 50 nM Lyzotracker Blue fluorophore (Invitrogen), 30 minutes of incubation. Before imaging, cells were thoroughly washed with a warm phosphate buffer (Gibco, ThermoFisher Scientific) to remove an excess of fluorophore and non-internalized nanoparticles or with Live Cell Imaging solution (Gibco, ThermoFisher Scientific) and observed under a fluorescent microscope at room temperature, without CO_2 control.

Fluorescence microscopy and microspectroscopy (FMS) in cells: Eu^{+3}-TiO_2 treated cell samples were excited by nonpolarized light from a Xe-Hg source (Sutter Lambda LS, Novato, CA) through broad-band filters (all band-pass filters and dichroic were BrightLine from Semrock, Rochester, NY). Fluorescence was detected through matching broadband filters as well. For spectral detection a narrow-band liquid-crystal tunable filter (LCTF; Varispec VIS-10-20 from CRi, Woburn, MA) was placed in front of an EMCCD camera (iXon3 897 from Andor, Belfast, UK), allowing sequential acquisition of images at different wavelengths within the transmission range of the emission filter. For each λ-stack of images, spectra from every volume-element of the field-of-view were extracted. An objective with 60x (water immersion) magnification was used with a high numerical aperture (NA = 1.27, working distance 0.17 mm). [36] The filters used in experiments were the following: for the nuclei or the lysosomes imaging 352-402 nm excitation, 409 nm dichroic, and 420-520 nm emission filters, for Eu^{+3}-TiO_2 nanoparticles imaging 430-460 nm excitation, 495 nm dichroic and 523-643 nm emission filters were used, and for the membrane imaging 430-460 nm excitation, 495 nm dichroic and 506-594 nm emission filters were used. Emission spectra were recorded with 5 nm scan step.

The local thermal heating of nanoparticles inside the cells, was obtained using a 1064 nm laser (Tweez 200si, Aresis) with a constant power of 200 mW. The center of a laser beam was placed on the Eu^{+3}-TiO_2 nanostructure inside the cell. Manual switching t_{on} = 5 seconds, t_{off} = 10 seconds approximately was used for manipulation of the laser, repeatedly. Measured fluorescence intensity data were normalized to initial intensity of 5%Eu^{+3}-TiO_2 nanostructure before heating. The temperature calibration curve (Equation 1), which presents the thermometer sensitivity (see supplementary data for more details on the calibration curve), was used for transformation of the fluorescence intensity in temperature difference (ΔT).

Confocal imaging: For confocal fluorescence microscopy imaging was used a custom made STED microscope from Abberior instruments, Germany, equipped with a UPLSAPO 60x/1.20 water immersion objective (Olympus Corporation, Japan) and a continuous-wave (CW) 561 nm and 640 nm laser with emission detected from 580-625 nm in one channel and from 655-720 in second channel. Gating was between 468 ps and 1.32 ns. Confocal images were taken with 100 nm pixel size scan resolution in a xy plane and as well as in xz and yz planes.

4.1 | Eu^{+3}-TiO_2 temperature dependent luminescence calibration

In pellets of Eu^{+3}-TiO_2 nanoparticle powder: For luminescence experiments, pellets were prepared from Eu^{+3}-TiO_2 powder. The luminescence spectra were obtained at front face configuration using a SPEX Fluorolog spectrofluorometer (0.22 m, Spex/1680) equipped with a Xe-lamp as the excitation source and a photomultiplier (Hamamatsu/R928) for detection, the excitation wavelength was 350 nm. The excitation spectra were corrected for the spectral distribution of the lamp intensity using a photodiode reference detector. The luminescence spectra were taken at different temperatures using a Peltier cooling/heating homemade system equipped with a temperature controller AUTONICS model TZN4S, with resolution of 0.10K.[44]

In water dispersions of Eu^{+3}-TiO_2 nanoparticles with a fluorescence microscope: The Eu^{+3}-TiO_2 nanoparticle powder was dispersed in distilled water using a water bath sonicator (Branson 2510), 10 μL of dispersion was placed in an 8 well cell chamber (Nunc, Labtek) and waited until dried to prevent particle movement during measurements. 300 μL of additional distilled water was added to the well to prevent temperature rise of the whole sample. The temperature was varied by a heater in a form of an objective-ring, which can heat up the sample precise enough without severe vertical gradients when using a water immersion objective needed for higher magnifications, which is in a contact with a sample holder. Before recording the fluorescence intensity at five different temperatures (20°C, 26°C, 30°C, 36°C, 37°C, all points with ±0.5°C) (Figure S9), we waited at least for 5 minutes to achieve the target temperature. For excitation 430-460 nm, 495 nm dichroic and 523-643 nm filters were used for emission detection. The measurement of the widefield fluorescence intensity in each pixel of the whole image was used to obtain a temperature calibration curve. The same fluorescence microscope was used for the cell experiments.[36]

In water dispersions of Eu^{+3}-TiO_2 with spectrofluorometer: Spectral measurements were performed on a spectrofluorometer Tecan Infinite M1000 (Tecan Group Ltd., Männedorf, Switzerland) using a black 96-well plate. 50 mg of Eu^{+3}-TiO_2 in 40 μL of a distilled water was placed in a well and waited for a day to settle. Measurements were done at three different temperatures (20°C, 30°C, 40°C) with thermal stabilization period of 30 minutes at each temperature step. Emission spectra were detected from 400-750 nm with excitation at 396 nm at each temperature, with 1 nm scan. Fluorescence intensity of spectral maximum peak at 615 nm was used to obtain temperature calibration curve.

ACKNOWLEDGMENTS

This work was financially supported by Helmholtz-Zentrum Berlin (HZB) and by the project CALIPSOplus under the Grant Agreement 730872 from the EU Framework Programme for Research and Innovation HORIZON 2020 and by the Belgian Fund for Scientific Research under the FRFC contract CDR J001019. CB is a Research Associate of the National Funds for Scientific Research (FRS-FNRS, Belgium). Dr. Maja Garvas and Ms. Selene Acosta contributed equally to this work.

REFERENCES

1. G. N. Somero, *Annu. Rev. Physiol.* **1995**, *57*, 43.
2. R. Brown, P. Rickless, *P. Roy. Soc. B-Biol. Sci.* **1949**, *136*, 110.
3. J. R. Hazel, E. E. Williams, *Prog. Lipid Res.* **1990**, *29*, 167.
4. A. M. Stark, S. Way, *Cancer* **1974**, *33*, 1664.
5. R. N. Lawson, M. S. Chughtai, *Can. Med. Assoc. J.* **1963**, *88*, 68.
6. A. T. Maurelli, P. J. Sansonetti, *PNAS USA* **1988**, *85*, 2820.
7. M. Karnebogen, D. Singer, M. Kallerhof, R. H. Ringert, *Thermochim. Acta* **1993**, *229*, 147.
8. X. D. Wang, O. S. Wolfbeis, R. J. Meier, *Chem. Soc. Rev.* **2013**, *42*, 7834.
9. G. Kucsko, P. C. Maurer, N. Y. Yao, M. Kubo, H. J. Noh, P. K. Lo, H. Park, M. D. Lukin, *Nature* **2013**, *500*, 54.
10. D. Jaque, F. Vetrone, *Nanoscale* **2012**, *4*, 4301.
11. M. G. Nikolić, Ž. Antić, S. Ćulubrk, J. M. Nedeljković, M. D. Dramićanin, *Sensor Actuat. B-Chem.* **2014**, *201*, 46.
12. A. Benayas, B. del Rosal, A. Pérez-Delgado, K. Santacruz-Gómez, D. Jaque, G. A. Hirata, F. Vetrone, *Adv. Opt. Mater.* **2015**, *3*, 687.
13. I. E. Kolesnikov, E. V. Golyeva, A. A. Kalinichev, M. A. Kurochkin, E. Lähderanta, M. D. Mikhailov, *SensorActuat. B-Chem.* **2017**, *243*, 338.
14. G. W. Walker, V. C. Sundar, C. M. Rudzinski, A. W. Wun, M. G. Bawendi, D. G. Nocera, *Appl. Phys. Lett.* **2003**, *83*, 3555.
15. D. Ross, M. Gaitan, L. E. Locascio, *Anal. Chem.* **2001**, *73*, 4117.
16. L. Marciniak, K. Prorok, L. Frances-Soriano, J. Perez-Prieto, A. Bednarkiewicz, *Nanoscale* **2016**, *8*, 5037.
17. C. Gota, K, Okabe, T. Funatsu, Y. Harada, S. Uchiyama, *J. Am. Chem. Soc.* **2009**, *131*, 2766.
18. S. Uchiyama, N. Kawai, A. P. de Silva, K. Iwai, *J. Am. Chem. Soc.* **2014**, *126*, 3032.
19. S. S. Syamchand, G. Sony, *J. Lumin.* **2015**, *165*, 190.
20. Y. H. Wang, T. F. Tian, X. Q. Liu, G. Y. Meng, *J. Membrane Sci.* **2006**, *280*, 261.
21. J. Reszczyńska, T. Grzyb, J. W. Sobczak, W. Lisowski, M. Gazda, B. Ohtani, A. Zaleska, *Appl. Surf. Sci.* **2014**, *307*, 333.
22. A. Cadiau, C. D. Brites, P. M. Costa, R. A. Ferreira, J. Rocha, L. D. Carlos, *ACS nano* **2013**, *7*, 7213.
23. S. W. Allison, G. T. Gillies, *Rev. Sci. Instrum.* **1997**, *68*, 2615.
24. V. Kiisk, I. Sildos, S. Lange, V. Reedo, T. Tätte, M. Kirm, J. Aarik, *Appl. Surf. Sci.* **2015**, *247*, 412.
25. R. Carbone, I. Marangi, A. Zanardi, L. Giorgetti, E. Chierici, G. Berlanda, A. Podestà, F. Fiorentini, G. Bongiorno, P. Piseri, P. G. Pelicci, P. Milani, *Biomaterials* **2006**, *27*, 3221.
26. Y. Wang, C. Wen, P. Hodgson, Y. Li, *J. Biomed. Mater. Res. Part A* **2014**, *102*, 743.

27. M. Garvas, A. Testen, P. Umek, A. Gloter, T. Koklic, J. Strancar, *PLoS One* **2015**, *10*, e0129577.
28. C. Bouzigues, T. Gacoin, A. Alexandrou, *ACS nano* **2011**, *5*, 8488.
29. K. Pawar, G. Kaul, *Adv. Sci. Eng. Med.* **2013**, *5*, 11.
30. C. R. Patra, S. S. A. Moneim, E. Wang, S. Dutta, S. Patra, M. Eshed, P. Mukherjee, A. Gedanken, V. H. Shah, D. Mukhopadhyay, *Toxicol. Appl. Pharmacol.* **2009**, *240*, 88.
31. V. S. Bollu, S. K. Nethi, R. K. Dasari, S. S. N. Rao, S. Misra, C. R. Patra, *Nanotoxicology* **2016**, *10*, 413.
32. H. Liu, C. Zhang, Y. Tan, J. Wang, K. Wang, Y. Zhao, G. Jia, Y. Hou, S. Wang, J. Zhang, *J. Nanopart Res.* **2014**, *16*, 2303.
33. S. Sandoval, J. Yang, J. G. Alfaro, A. Liberman, M. Makale, C. E. Chiang, I. K. Schuller, A. C. Kummel, W. C. Trogler, *Chem. Mater.* **2012**, *24*, 4222.
34. M. Tan, G. Wang, Z. Ye, J. Yuan, *J. Lumin.* **2006**, *117*, 20.
35. C. J. Howard, T. M. Sabine, F. Dickson, *Acta Crystalogr. Sec. B: Struc. Sci.* **1991**, *42*, 462.
36. M. Rutar, N. Rozman, M. Pregelj, C. Bittencourt, R. C. Korošec, A. S. Škapin, A. Mrzel, S. D. Škapin, P. Umek, *Beilstein J. Nanotechnol.* **2015**, *6*, 831.
37. Z. Arsov, I. Urbančič, M. Garvas, D. Biglino, A. Ljubetič, T. Koklič, J. Štrancar, *Biomed. Opt. Express* **2011**, *2*, 2083.
38. I. Urbančič, M. Garvas, B. Kokot, H. Majaron, P. Umek, H. Cassidy, M. Škarabot, F. Schneider, S. Galiani, Z. Arzov, T. Kloklič, D. Matallanas, M. Čeh, I. Muševič, C. Eggeling, J. Štrancar, *Nano Letters* **2018**, *18*, 5294.
39. Ž. Antić, R. M. Krsmanović, M. G. Nikolić, M. Marinović-Cincović, M. Mitrić, S. Polizzi, M. D. Dramićanin, *Mater. Chem. Phys.* **2012**, *135*, 1064.
40. P. Guttmann, C. Bittencourt, S. Rehbein, P. Umek, X. Ke, G. Van Tendeloo, C. P. Ewels, G. Schneider, *Nat. Photonics* **2012**, *6*, 25.
41. P. Guttmann, S. Werner, F. Siewert, A. Sokolov, J. S. Schmidt, M. Mast, M. Brzhezinskaya, C. Jung, R. Follath, G. Schneider, *Microsc. Microanal.* **2018**, *24*, 204.
42. C. Bittencourt, S. Werner, C. Haebel, P. Guttmann, M. Sluban, P. Umek, P. Kruger, *Microsc. Microanal.* **2018**, *24*, 474.
43. S. Pajk, M. Garvas, J. Štrancar, S. Pečar, *Org. Biomol. Chem.* **2011**, *9*, 4150.
44. L. J. Borrero-González, S. Acosta, C. Bittencourt, M. Garvas, P. Umek, L. A. O. Nunes, *Optical Mater.* **2020**, *101*, 109770.

SUPPORTING INFORMATION

Additional supporting information may be found online in the Supporting Information section at the end of the article.

How to cite this article: Garvas M, Acosta S, Urbančič I, et al. Single cell temperature probed by Eu^{+3} doped TiO_2 nanoparticles luminescence. *Nano Select*. **2021**;*2*:1208–1217.
https://doi.org/10.1002/nano.202000207